The Journal of Neuroscience, May 1994, 14(5): 2789–2799

Overexpression of a Potassium Channel Gene Perturbs Neural Differentiation

Susan M. Jones and Angeles B. Ribera

Department of Physiology, University of Colorado Health Sciences Center, Denver, Colorado 80262

Functional regulation of potassium currents in developing neurons is pivotal for changes in excitability and action potential waveform. Here, we test whether an excess of potassium channel transcripts is sufficient to drive functional expression of potassium current and shortening of the duration of the action potential. Injection of *Shaker*-like potassium channel transcripts into two-cell stage embryos achieves increases in RNA levels. The elevated levels of potassium channel RNA produce larger delayed-rectifier currents. Action potential durations are briefer, indicating that larger potassium currents are not compensated by changes in inward currents. Strikingly, overexpression of potassium current RNA leads to a reduction in the number of morphologically differentiated neurons in culture. We suggest that, by prematurely reducing the duration of the impulse, early overexpression of potassium channel activity suppresses normal developmental cues.

[Key words: action potential modulation, delayed-rectifier potassium current,* Shaker*-like potassium channel, neuronal differentiation, RNA overexpression,* Xenopus *embryo]

Electrically excitable membranes serve multiple functions in the nervous system. In addition to rapid signaling, action potentials initiate biochemical cascades required for synaptic plasticity in the adult and for programs of differentiation during embryonic development (Spitzer, 1994). Primary amphibian neurons acquire electrical excitability within 8 hr of their last round of DNA synthesis (Warner, 1973; Baccaglini and Spitzer, 1977; Lamborghini, 1980; Hartenstein, 1989). Initial action potentials are of long duration, are calcium dependent, and occur spontaneously in immature amphibian spinal neurons (Holliday and Spitzer, 1990). Long-duration impulses provide significant elevations of intracellular cytosolic and nuclear calcium (Holliday et al., 1991). These calcium transients provide signals necessary for subsequent elaboration of several characteristics, including neurite outgrowth, formation of neuron–myocyte contacts, accumulation of GABA-like immunoreactivity, and acceleration of potassium current kinetics (Bixby and Spitzer, 1984; Henderson et al., 1984; Holliday and Spitzer, 1990, 1993; Desarmenien and Spitzer, 1991; Holliday et al., 1991).

The impulse duration and associated calcium influx are developmentally regulated by a delayed-rectifier potassium current (Barish, 1986; O'Dowd et al., 1988). A small current characterizes immature neurons and permits impulses to be of long duration. Increases in its density convert the action potential to a brief sodium-dependent spike. The normal increase in delayed-rectifier potassium current and shortening of impulse duration require transcription during an early critical period, indicating that functional expression of potassium current is under transcriptional control.

The functional significance of potassium current maturation motivates identification of the molecular genetic basis for regulation of its expression in developing neurons. Splice variants and the existence of four distinct gene subfamilies (*Shaker, Shab, Shaw,* and *Shal*) contribute to the structural and functional diversity of potassium channels (for reviews, see Jan and Jan, 1992; Ribera and Spitzer, 1992; Salkoff et al., 1992). In addition, different potassium channels localize and function independently within neurons (Baker and Salkoff, 1990; Covarrubias et al., 1991; Sheng et al., 1992; Wu and Barish, 1992).

The genetic regulation of potassium channel functional expression has been analyzed in invertebrate systems. The size of the A-current encoded by the *Shaker* gene in *Drosophila* flight muscle is a linear function of gene dosage within the range of zero to two gene copies; addition of more than two copies, however, has little effect on current size (Timpe and Jan, 1987; Haugland and Wu, 1990). Similarly, injection of the *Aplysia* AK01a potassium channel minigene into identified *Aplysia* neurons induces large voltage-dependent potassium currents whether or not the injected neuron normally expresses the AK01a potassium channel (Kaang et al., 1992). As in *Drosophila* flight muscle, the extent to which an increase in gene copy number produces functional overexpression appears to be nonlinear, since only 10^7 copies of the channel are induced by injection of $0.3–6 \times 10^{14}$ copies of the minigene.

Much less information exists about the genetic control of potassium channel functional expression in developing nervous systems, where they modulate the duration of the impulse and other aspects of excitability (Ribera and Spitzer, 1992). Previous work indicates that functional maturation of potassium current requires new RNA synthesis during a critical period (Ribera and Spitzer, 1989). This finding is consistent with the hypothesis that normal differentiation of potassium current is controlled primarily by developmentally regulated levels of potassium channel RNA. Here, we test this possibility directly by injecting *in vitro* synthesized potassium channel RNA into cleavage stage

Received June 21, 1993; revised Oct. 13, 1993; accepted Oct. 26, 1993.

We thank Alison Hofmann, Dick Kennedy, Janet Lieber, and George Tarver for expert technical assistance, Dr. Devorah Gurantz for computer programs, Drs. Richard Aldrich and Roderick MacKinnon for suggesting the use of and providing the WF potassium channel mutant, and Drs. Paul Fuchs and Rock Levinson for comments on the manuscript. This work was supported by Training Grant NS07083, NRSA Postdoctoral Fellowship NS09237 (S.M.J.), and NIH Grants RO1-NS25217 and KO4-NS01531 (A.B.R.). A.B.R. is a Fellow in Neurosciences of the Klingenstein Foundation and a Basil O'Connor Scholar of the March of Dimes Foundation.

Correspondence should be addressed to Angeles B. Ribera, Department of Physiology, C-240, University of Colorado Health Sciences Center, Denver, CO 80262.

Table 1. Survival of RNA- and tracer-injected embryos

Type of injection	Number of experiments analyzed	Number of embryos examined	% survival[a] (mean ± SD)
None	13	1441	84 ± 11
Tracer alone	57	1762	87 ± 7
Tracer + XSha1 RNA[b]	69	2812	80 ± 7
Tracer + XSha2 RNA[b]	4	204	77 ± 22
Tracer + WF RNA[b]	4	200	92 ± 14
Tracer + β-galactosidase RNA[b]	7	142	93 ± 11

[a] Percentage survival for injected embryos was assessed as the number of live embryos at stages 10–15 divided by the number of embryos injected at the two-cell stage. Percentage survival for uninjected embryos was assessed as the number of live embryos at stages 10–15 divided by the number of embryos present at the two-cell stage.

[b] 60–100 pg/nl injected RNA.

Xenopus embryos. This perturbation results in early functional overexpression of potassium currents, indicating that immature neurons are capable of making larger potassium currents. The density of the overexpressed potassium current predicts directly the duration of the impulse. In addition, functional overexpression of potassium currents leads to a dramatic reduction in the appearance of morphologically identifiable neurons.

Materials and Methods

Animals and cell culture. Embryos were produced by standard *in vitro* fertilization techniques (Moon and Christian, 1989) and staged according to Nieuwkoop and Faber (1967). Neural plate stage (stage 15; 17.5 hr) cultures were prepared as described previously (Spitzer and Lamborghini, 1976; Blair, 1983; Ribera and Spitzer, 1989) from the posterior two-thirds of the neural plate, which comprise the future spinal cord and hindbrain (Eagleson and Harris, 1990). Early or young and mature or late refer to data obtained from neurons 6–9 hr (stages 22–25) and 18–30 hr in culture (stages 30–34), respectively. By 18 hr in culture, the delayed-rectifier potassium current recorded from primary neurons has undergone the full extent of its maturation (Ribera and Spitzer, 1989).

RNA synthesis and injections. The entire coding regions of the XSha1 and XSha2 potassium channel genes were cloned into the pSP64T vector (Melton et al., 1984) to flank it with 5′ and 3′ untranslated regions of β-globin. These untranslated sequences confer stability and efficient expression upon exogenously introduced RNA (Moon and Christian, 1989). The cloning of XSha1 was as described previously (Ribera and Nguyen, 1993). For XSha2, the coding region was excised from a pSP73 recombinant (Ribera, 1990) using HindIII and PstI and blunt ended with Klenow. The pSP64T vector was cut with BglII and treated with Klenow to yield compatible ends. The resulting recombinant pSP64T was linearized with SmaI. Capped sense RNA was generated by *in vitro* transcription with SP6 RNA polymerase in the presence of rNTPs and cap analog (Boehringer-Mannheim, Indianapolis, IN).

Introduction of RNA into developing embryos was achieved by injection into one side of the animal pole immediately after first cleavage (Moon and Christian, 1989). Typically, 5–10 nl of injection solution was pressure injected (2–3 psi for 2–3 sec) using fine drawn micropipettes (~10 μm tip diameter; Narashige USA, Inc., Greenvale, NY). The injection solution contained a lineage tracer (20–30 mg/ml; rhodamine-conjugated dextran; Molecular Probes, Eugene, OR) and the desired RNA (5–200 pg/nl). The coinjected dextran was pretreated to remove RNAase contamination by boiling for 10 min in 0.1% diethyl pyrocarbonate followed by methanol precipitation (recommendation of Josh Stahl, Molecular Probes).

Injection of one cell of the two-cell stage embryo permitted half of the embryo to serve as an uninjected internal control. Survival rates of tracer-injected and noninjected embryos from the same clutch are similar (Table 1). On the basis of external morphological criteria, the injected embryos undergo normal gastrulation movements. Further, common defects arising after injection of other RNAs (e.g., kinking, epidermal, and axial abnormalities; Moon and Christian, 1989) are not correlated with injection of XSha1 RNA into cleavage stage embryos.

Since the injected XSha1 RNA has the typical half-life of 6–8 hr (Harland and Mischer, 1988; Kintner, 1988; data not shown), following injection of 400 pg of RNA at the two-cell stage (~1.5 hr), embryos contain ~80,000 cells and ~80 pg of RNA at the time of dissection in preparation for culture. The amount of exogenous RNA in each cell of the injected side of the embryo is estimated as ~1 fg or 1000 copies. This calculation is based upon a simplification that RNA is partitioned equally at each cellular division and that the same number of divisions occur for cells of different lineages.

Whole-mount in situ *hybridization.* The nonradioactive detection method using digoxigenin-labeled probes (Harland, 1991) was followed with minor modifications. Injected pigmented embryos were fixed in MEMPFA (4% paraformaldehyde, 0.1 M MOPS, pH 7.4, 1 mM $MgSO_4$, 2 mM EGTA) for 12–15 hr at 4°C. Hybridization was carried out overnight. After incubation with antibody, washes were carried out over ≥24 hr with a minimum of seven changes. The alkaline phosphatase reaction product was developed in the presence of nitro blue tetrazolium/5-bromo-4-chloro-3-indoyl phosphate for ~2 hr, a condition that does not permit detection of the endogenous XSha1 mRNA signal in either whole-mount or sectioned embryos (Ribera and Nguyen, 1993). Whole-mount embryos were embedded in Eponate 12 (Pella, Redding, CA) and sectioned at 10 μm. Sections were viewed with either bright-field optics or epifluorescent illumination, and photography was done with TMAX 400 film.

Biophysical methods and analyses. Whole-cell gigaohm recording methods were employed (Hamill et al., 1981). An Axopatch 1-C amplifier (Axon Instruments, Foster City, CA) was used in conjunction with a TL-1 data interface (Axon Instruments), pCLAMP computer programs (Axon Instruments), and a 386 PC computer clone for acquisition of data. Neurons were identified on the basis of morphology, and those with short processes (<50 μm) were selected (O'Dowd et al., 1988) to avoid inadequate control of the membrane voltage. Electrodes were pulled (Flaming/Brown, Sutter Instruments, Novato, CA) from borosilicate glass (Drummond Scientific Co., Broomall, PA) and had resistances ranging between 2 and 4 MΩ when filled with the standard pipette solution (100 mM KCl, 10 mM EGTA, 10 mM HEPES, pH 7.4).

Action potentials were recorded with whole-cell electrodes by switching to current clamp. A steady level of current was injected to hold the membrane potential near −80 mV, and impulses were elicited by injecting brief depolarizing current pulses. For these experiments, cells were bathed in a standard saline solution (in mM): NaCl, 125; KCl, 3; $CaCl_2$, 10; HEPES, 5; pH 7.4.

For recording of whole-cell potassium currents, the bath saline consisted of (in mM) NaCl, 80; KCl, 3; $MgCl_2$, 5; $CoCl_2$, 10; HEPES, 5; pH 7.4. Sodium currents were blocked by addition of 10^{-6} M tetrodotoxin (Sigma); calcium currents were avoided by omission of calcium chloride from the saline and addition of 10 mM cobalt chloride. For recording of inward sodium and calcium currents, pipettes were filled with (in mM) CsCl, 100; tetraethylammonium-Cl (TEA), 10; EGTA, 10; HEPES, 10; pH 7.4 with CsOH. Sodium currents were recorded in the absence of tetrodotoxin and addition of 40 mM TEA to the bath. Data were accepted when the sodium current activated and inactivated smoothly. Calcium current was recorded in the presence of tetrodotoxin and 10 mM $CaCl_2$; $MgCl_2$ and $CoCl_2$ were omitted from the bath. The capacitative transient was electronically nulled prior to establishment of the whole-cell configuration. Membrane potential was usually held at −80 mV and stepped to depolarized voltages ranging between −45 and 105 mV in increments of 5 or 10 mV for 20–200 msec. The currents elicited were digitized at 100 μsec.

Cell capacitance and series resistance were determined from the capacitative current transient recorded after break in when sampling at 20 μsec intervals. The cell capacitance was used to evaluate the membrane surface area (1 μF/cm²) for normalization of current amplitude to density. The series resistance value was used to estimate the associated voltage error (see below). Leak subtraction was accomplished using a modified *P*/4 protocol with 11 hyperpolarizing subpulses (pCLAMP, Axon Instruments). Evaluation of current densities, series and input resistances, and cell capacitances was aided by programs written and generously provided by Dr. Devorah Gurantz (UCSD). Measurement of times to peak or half-maximum current and of percentage inactivation was accomplished with the CLAMPFIT program (pCLAMP). Data are presented as mean ± SEM. The Student's *t* test (one-tail) was used to evaluate the degree of significant difference between data sets; a *p* value of less than 0.05 was considered indicative of statistical significance. Conductance densities were calculated by dividing current densities by driving force, with a calculated potassium equilibrium potential of −86 mV. Steady-state activation parameters were evaluated only for re-

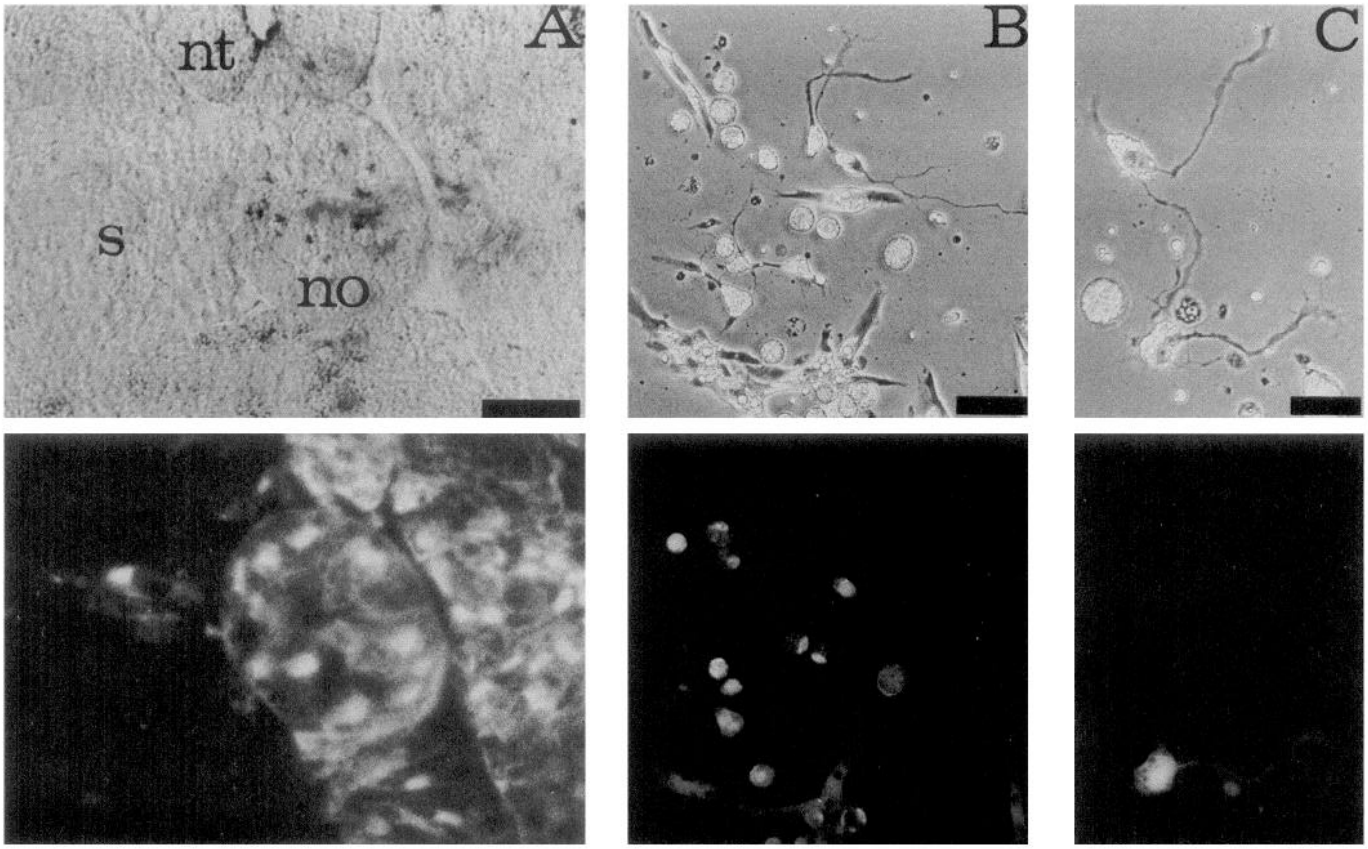

Figure 1. Fluorescence identifies cells derived from a single injected blastomere. *A*, Fluorescence due to the presence of the lineage tracer (*bottom*) is primarily restricted to the right side of the embryo and present within the neural tube. Further, the distribution of exogenous XSha1 RNA is visualized by the reaction product following *in situ* hybridization using digoxigenin-labeled probes (*top*). The section was viewed with either bright-field optics (*top*) or rhodamine epifluorescent illumination (*bottom*). The embryo was coinjected with rhodamine-conjugated dextran and XSha1 RNA at the two-cell stage, fixed at stage 24, processed as a whole-mount for *in situ* hybridization of XSha1 RNA (Harland, 1991; Ribera and Nguyen, 1993), embedded in plastic, and transversely sectioned at 10 μm. The incubation with the alkaline phosphatase substrates (NBT and BCIP) was carried out for only 2 hr; an 8 hr incubation is required to reveal the endogenous XSha1 mRNA signal. Longer incubation times reveal a greater distribution of XSha1 RNA, suggesting that the delivery of RNA to progeny of the injected cell is not uniform. *nt*, neural tube; *s*, somites; *no*, notochord. *B*, A neural plate culture was prepared from a stage 15 embryo that had one cell injected at the two-cell stage with solution containing rhodamine-conjugated dextran. With phase-contrast optics (*top*), neuronal cell bodies appear phase bright due to the normal inclusions of yolk platelets and lipid granules; processes are phase dark. Rhodamine epifluorescent illumination (*bottom*) demonstrates that the fluorescent lineage tracer is present in approximately half of all cell types in culture, including neurons, myocytes, and morphologically undifferentiated cells. The culture was examined at 1 d in culture. *C*, Two neurons in culture viewed at higher magnification. Only one is fluorescent, and the tracer is present in the process. The culture was examined at 1 d in culture. Scale bars: *A*, 150 μm; *B*, 100 μm; *C*, 25 μm.

cordings in which the conductance reached a plateau. The equation $G = G_{max}/1 + \exp(V_{1/2} - V/k)$ was fitted to the data (G_{max}, maximal conductance; $V_{1/2}$, voltage of half-activation; k, slope factor).

Current and conductance density–voltage plots have been mathematically corrected for the voltage error introduced by the series resistance. After voltages had been corrected for series resistance errors, they were binned into groups at 5 mV intervals. Within a group (e.g., 24 hr fluorescent) and after correction, the absolute magnitude of the current did not affect $t_{1/2}$ values, which indicates the appropriateness of the correction. The extents of voltage errors were similar for fluorescent and nonfluorescent cells. Electronic compensation was used in initial experiments, and comparisons of data from the same cell when the series resistance error was corrected for either electronically or mathematically indicated that I–V curves constructed after either method of compensation were the same.

Examination of cell cultures and cell counting. Cultures were viewed on a Nikon Diaphot microscope with phase-contrast optics or rhodamine epifluorescent illumination. Neurons and myocytes were identified on the basis of morphological criteria (Henderson and Spitzer, 1986; O'Dowd et al., 1988; Ribera and Spitzer, 1991) and scored for rhodamine fluorescence. Visualization of the fluorescence did not interfere with cell survival or subsequent differentiation. Data are expressed as the ratio of the number of fluorescent to nonfluorescent morphologically identified cells in a culture prepared from a single neural plate. Only cultures that had greater than 10 and 50 nonfluorescent morphologically identifiable neurons and myocytes, respectively, and no obvious signs of bacterial contamination were included; these criteria did not result in the elimination of more cultures prepared from RNA-injected embryos. Statistical analysis of the difference between mean ratio values was done with the nonparametric Mann–Whitney test (two-tail), and p values of less than 0.05 were considered indicative of a statistically significant difference.

Results

Fluorescent tracer permits identification of live neurons derived from an injected cell

Coinjection of embryos with lineage tracer and RNA does not impair embryonic survival (Table 1). In 1–2-d-old embryos the lineage tracer is restricted to either the right or left side (Fig. 1*A*), consistent with each cell of a first cleavage stage embryo giving rise to the majority of the right or left side of the embryo (Klein, 1987).

The XSha1 gene encodes a delayed rectifier–type potassium current, and its mRNA is found within a subset of primary spinal neurons, sensory Rohon-Beard cells (Ribera and Nguyen,

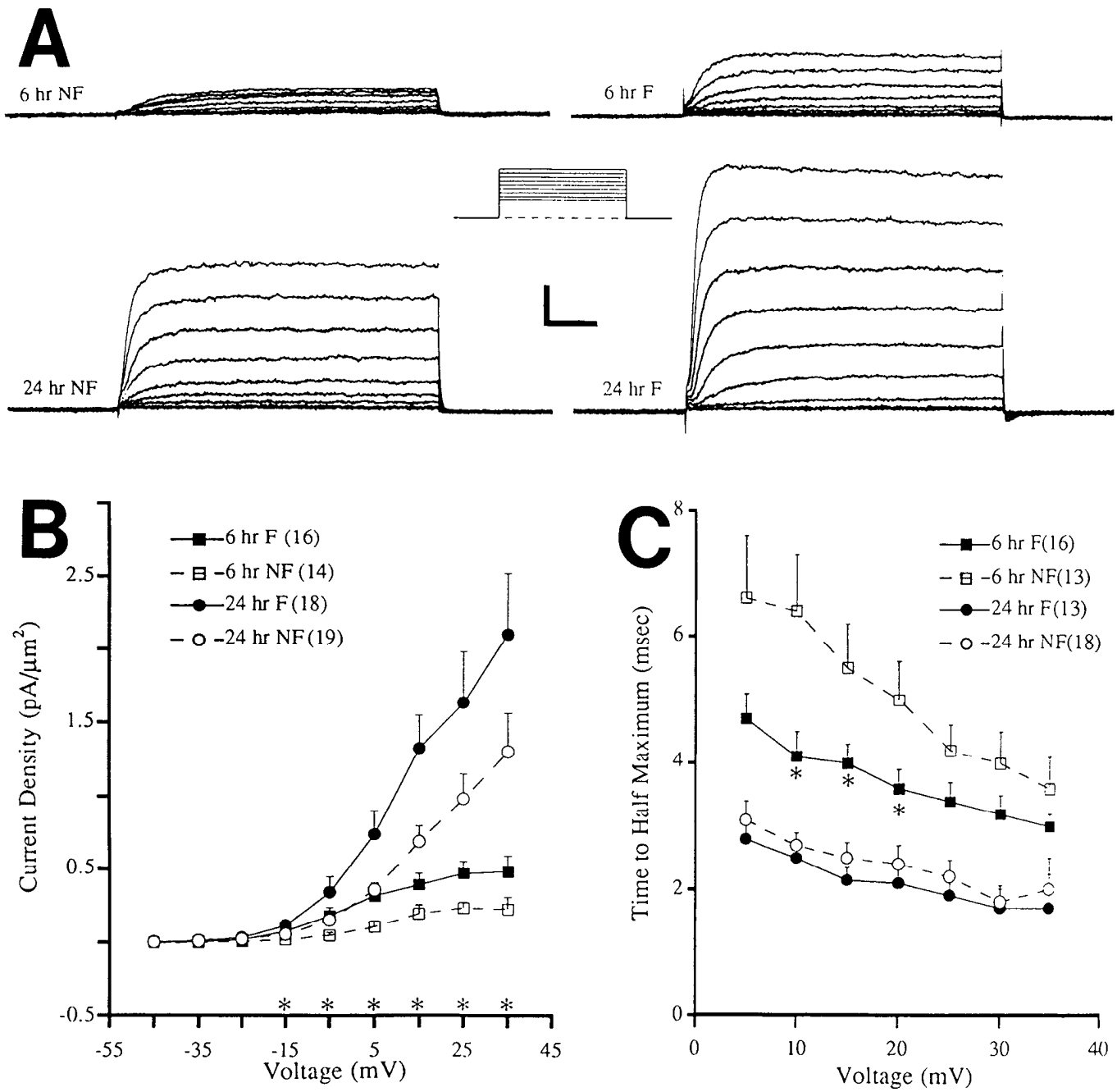

Figure 2. Elevation of potassium channel RNA levels suffices to produce larger and faster potassium currents. *A*, Delayed-rectifier potassium currents recorded from neurons: 6–9 hr (*top*) 22–26 hr (*bottom*) in culture. Neurons were held at −80 mV and stepped to voltages ranging between −45 and +35 mV in 10 mV increments. Currents recorded from fluorescent (*F*) neurons (*right*) are larger than those recorded from nonfluorescent (*NF*) neurons (*left*) although capacitance values are similar (20 pF, 6 hr NF; 21 pF, 6 hr F; 21 pF, 24 hr NF; 25 pF, 24 hr F). Cultures were prepared from embryos that had been injected with 80 pg/nl XSha1 RNA. Calibration: 1000 pA, 10 msec. *B*, Current density as a function of voltage. In both young and mature neurons, larger potassium current densities are found in fluorescent than in nonfluorescent cells. *Asterisks* indicate that differences between fluorescent and nonfluorescent data, at both early and late times, are statistically significant at the designated voltages; p values range between 0.007 and 0.05. *C*, Time to half-maximum current as a function of voltage. In young neurons, potassium currents activate more rapidly in fluorescent than in nonfluorescent neurons. *Asterisks* indicate that the differences between fluorescent and nonfluorescent data at early times are statistically significant at the designated voltages; p values range between 0.008 and 0.035.

1993). Microinjection of two-cell stage embryos with *in vitro* synthesized XSha1 RNA leads to elevated levels of its RNA in 1- and 2-d-old embryos (Fig. 1*A*). The distribution of coinjected XSha1 RNA overlaps with the fluorescence signal. Similar results are found for coinjected β-galactosidase RNA (data not shown), suggesting that dextran traces the disposition of a coinjected RNA as well as lineage. Further, the exogenous XSha1 RNA is observed in the neural tissue. The continued presence of coinjected XSha1 RNA in a stage 25 (~1 d) embryo is consistent with a 6–8 hr half-life (Harland and Mischer, 1988; Kintner, 1988; data not shown). These findings indicate that the embryo injection protocol delivers RNA to the tissue of interest and it persists to the appropriate time.

In cultures prepared from neural plate stage embryos (stage

Table 2. Properties of sodium current in fluorescent and nonfluorescent neurons

	Young		Mature	
	Fluorescent[a] (10)	Nonfluorescent (12)	Fluorescent[a] (7)	Nonfluorescent (7)
Voltage of peak current (mV)	17 ± 2	8 ± 3	19 ± 4	19 ± 3
Time to peak current (msec)	1.1 ± 0.1	1.2 ± 0.1	1.3 ± 0.1	1.3 ± 0.1
Peak current density (pA/μm^2)	−0.7 ± 0.1	−0.6 ± 0.1	−1.7 ± 0.2	−1.6 ± 0.1

Numbers in parentheses represent number of neurons.
[a] 80 pg/nl injected XShal RNA.

15, 17.5 hr), the tracer is found in all cell types, including neurons, myocytes, and morphologically undifferentiated cells (Fig. 1*B,C*). A similar strategy has been employed to trace *Xenopus* cells in culture that had received exogenous synapsin I by injection of cleavage stage embryos (Lu et al., 1992).

Overexpression of XShal RNA leads to increased potassium current densities

It is known that differentiation of potassium current requires synthesis of new mRNA during an early critical period (Ribera and Spitzer, 1989). Does the critical mRNA encode the potassium channel or a required regulatory factor? This issue was examined at the cellular level with whole-cell voltage-clamp recording techniques. The properties of currents recorded from nonfluorescent neurons confirm previous results obtained from neurons in cultures prepared from uninjected embryos (Ribera and Spitzer, 1989; Desarmenien and Spitzer, 1991), demonstrating that nonfluorescent cells serve as internal controls. At both early and late times in culture, the densities of sustained potassium currents are two- to threefold larger in fluorescent neurons (Fig. 2*A,B*), consistent with epitope tagging experiments that indicate that protein translated from injected XShal RNA is present at these times (data not shown). The larger outward currents recorded from fluorescent neurons do not show a change in the reversal potential of tail currents or an increased extent of inactivation, indicating that sustained outward potassium currents are induced. The effect of potassium channel RNA overexpression is specific, since sodium and calcium current densities, kinetics, and activation properties are unaffected (Table 2, Fig. 3). Further, the normal developmental increase in density of peak sodium current is observed in both fluorescent and nonfluorescent cells.

Kinetic differences are noted in currents recorded from fluorescent neurons (Fig. 2*A,C*). At early times, the current recorded from fluorescent neurons activates more rapidly than that from nonfluorescent cells; the time to half-maximum is significantly reduced by ~33%. The observed decrease in time to half-maximum at early times in fluorescent neurons is similar to the reduction in time to half-maximum normally observed with development (Harris et al., 1988; O'Dowd et al., 1988). Overexpression of XShal at late times, however, leads to no further reduction in the time to half-maximum.

In order to analyze steady-state properties of activation, conductance density–voltage plots were constructed by dividing current densities by the driving force (Fig. 4*A*). G_{max} values in fluorescent neurons are two- to threefold larger in fluorescent neurons at both early and late times. Comparisons between fluorescent and nonfluorescent cells of voltage sensitivities of steady-state activation are facilitated by normalizing conductance density values by division with G_{max} (Fig. 4*B*). Single Boltzmann equations fit data obtained from fluorescent and nonfluorescent cells at both early and late times. In fluorescent neurons, $V_{1/2}$ is ~5 mV more negative at early but not at late times (Fig. 4*B*). The smaller change in this parameter at late times may reflect the slight shift (~2 mV) in $V_{1/2}$ of the endogenous current at later times to more negative potentials.

Functional overexpression of XShal RNA results in briefer action potentials

Reconstruction of action potentials from whole-cell currents demonstrates that the density of delayed-rectifier potassium current serves as a sensitive index of impulse duration (Lockery and Spitzer, 1992). At early times, action potentials are briefer in fluorescent neurons (Fig. 5*A*). The effect is dependent upon the dose of injected RNA (Fig. 5*B*). For a dose of 80 pg/nl (~400 pg/embryo), the action potential duration is significantly reduced to 6.5 ± 1.1 (n = 10) from a control value of 66 ± 19 msec (n = 26; $p \leq 0.03$). Mathematical reconstruction of the impulse indicates that this degree of shortening would be the direct consequence of two- to threefold larger potassium currents (Fig. 2*B*; Lockery and Spitzer, 1992).

No difference is noted in durations of action potentials recorded from mature fluorescent and nonfluorescent cells. Computer simulations of action potentials indicate that, at this time, impulse durations are insensitive to changes in potassium current density within a 12-fold range (Lockery and Spitzer, 1992). At both early and late times, no differences are noted between fluorescent and nonfluorescent cells in the overshoot of the action potential or the current required to elicit an impulse (data not shown), consistent with the finding that other voltage-dependent currents involved in action potential generation are not affected (Fig. 3, Table 2). The durations of action potentials recorded from nonfluorescent neurons confirm previous results obtained from neurons in cultures prepared from uninjected embryos (Spitzer and Lamborghini, 1976; Blair, 1983; O'Dowd, 1983; Ribera and Spitzer, 1989). The normal developmental shortening of the action potential duration is observed in these neurons. These findings further support the use of cells that do not contain the lineage tracer as internal controls.

An alternative, indirect explanation for the shortening of impulse durations at early times is that injection of potassium channel RNA results in a general alteration of neuronal membrane properties. To address this possibility directly, we examined several indexes of membrane and recording properties including input and series resistances, cell capacitance (a measure of cell size), and resting membrane potential (Table 3). None of these parameters vary between fluorescent and nonfluorescent cells at either early or late times, confirming that the changes in the duration of the impulse at early times are due directly to functional overexpression of potassium current.

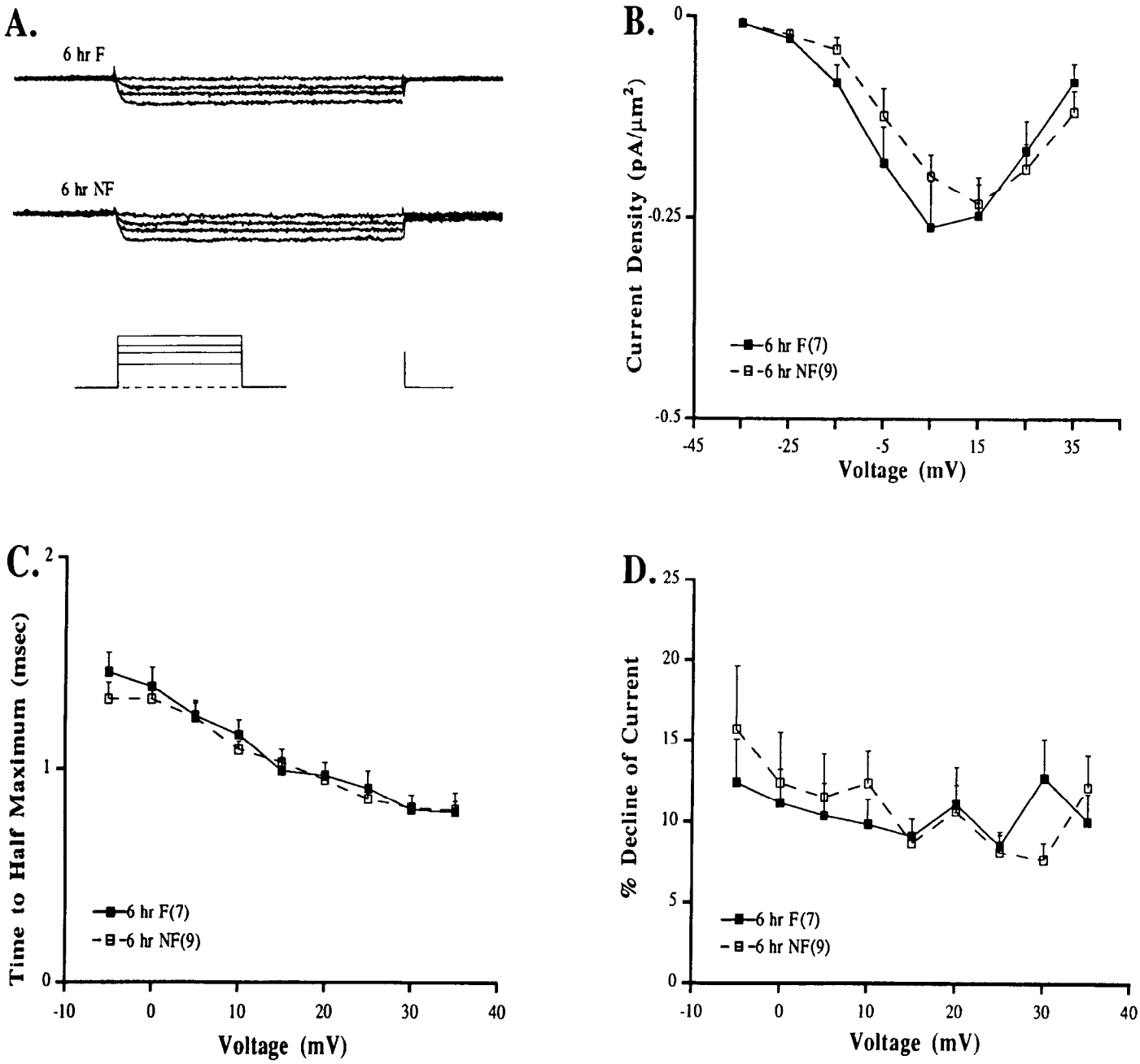

Figure 3. Calcium currents are unaffected by functional overexpression of XSha1 RNA. *A*, Calcium currents recorded from nonfluorescent (*bottom*) and fluorescent (*top*) young neurons. Capacitance values are similar (17 pF, 6 hr NF; 13 pF, 6 hr F). Neurons were held at −80 mV and stepped to command voltages of −30, −5, +10 and +30 mV. Cultures were prepared from embryos that had been injected with 80 pg/nl XSha1 RNA. Calibration: 500 pA, 10 msec. *B*, Calcium current density as a function of voltage is unaffected by overexpression of XSha1 RNA. *C*, Time to half-maximum calcium current as a function of voltage is similar for fluorescent and nonfluorescent neurons. *D*, Stimulus-dependent decay of calcium current does not differ between fluorescent and nonfluorescent cells. The percentage decline in calcium current was calculated by subtracting from 1 the ratio of the current amplitudes recorded at the end and at the peak of a 60 msec voltage step.

Elevated potassium channel RNA levels reduce the number of morphologically identifiable neurons

Calcium influx occurring during long-duration action potential impulses appears to be required for normal neuronal development (for review, see Holliday and Spitzer, 1991). Overexpression of potassium currents suppresses calcium-dependent action potentials and may thus perturb neuronal development. The numbers of morphologically differentiated fluorescent and nonfluorescent neurons in culture are compared to examine this possibility. A differentiation index, defined as the ratio of the number of fluorescent to the number of nonfluorescent morphologically identified neurons or myocytes, normalizes the data. This analysis focuses on these two morphologically differentiated cell types because the total number of cells in a culture dish is $>10^3$. However, the majority of cells (~90%) in culture are morphologically undifferentiated (Henderson and Spitzer, 1986) and therefore of unknown cell type. Further, their number varies greatly due to the inherent variability in dissection of tissue adjacent to the neural plate.

Since only one cell of a two-cell embryo is injected, the num-

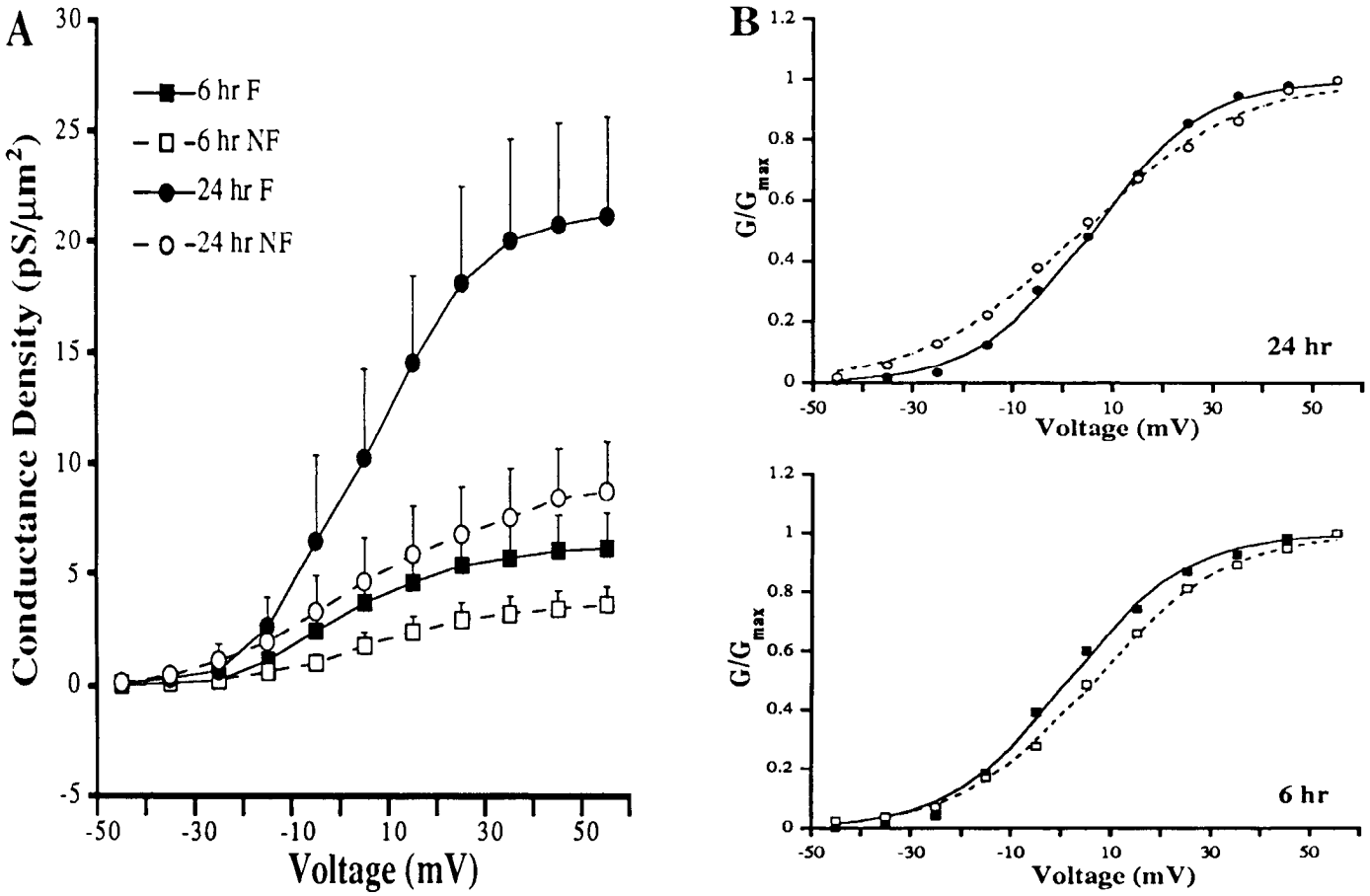

Figure 4. Functional overexpression of XSha1 RNA in the developing neuron produces potassium currents with altered steady-state activation properties. *A*, Conductance density as a function of voltage. Neurons were in cultures prepared from embryos injected with 80 pg/nl XSha1 RNA. G_{max} values for 6 hr nonfluorescent and fluorescent cells are 3.7 ± 0.8 (n = 12) and 6.2 ± 1.6 (n = 13) pS/μm², respectively; G_{max} values for 24 hr nonfluorescent (*NF*) and fluorescent (*F*) cells are 8.8 ± 2.2 (n = 7) and 21.2 ± 4.5 (n = 6) pS/μm², respectively. *B*, A single Boltzmann equation was fit to normalized data. *Bottom*: *6 hr NF*, $V_{1/2}$, 6.2 ± 0.4; k, 12.9 ± 0.3; χ^2, 0.16 × 10^{-3}; *6 hr F*, $V_{1/2}$, 1.3 ± 0.6; k, 11.4 ± 0.6; χ^2, 0.61 × 10^{-3}. *Top*: *24 hr NF*, $V_{1/2}$, 3.8 ± 0.7; k, 15.2 ± 0.6; χ^2, 0.48 × 10^{-3}; *24 hr F*, $V_{1/2}$, 5.6 ± 0.4; k, 10.9 ± 0.4; χ^2, 0.26 × 10^{-3}. At 6 hr, greater differences between the $V_{1/2}$ values of fluorescent and nonfluorescent cells are noted.

bers of fluorescent and nonfluorescent cells in culture are expected to be equal. When the fluorescent tracer is injected by itself, the mean differentiation index for morphologically differentiated neurons is ~1 (Fig. 6). Coinjection of XSha1 RNA with rhodamine-conjugated dextran leads to a dramatic and significant decrease in this index, indicating that the relative numbers of fluorescent neurons are decreasing (Fig. 6*A*). The effect is enhanced by increasing the concentration of injected XSha1 RNA and reaches a value of 0.12 for the highest dose of injected XSha1 RNA. Similar results are obtained by coinjection of tracer with RNA encoding another *Xenopus* potassium channel, XSha2.

The loss is restricted to fluorescent neurons and not a consequence of nonspecific actions on all neurons, because the average number of identifiable nonfluorescent neurons does not change when potassium channel RNA is injected at the two-cell stage. For cultures prepared from embryos injected with tracer only or tracer plus XSha1 RNA (80 pg/nl), the mean numbers of nonfluorescent neurons are 32 ± 2 (n = 65) or 30 ± 2 (n = 72), respectively.

Although the effect is specific to fluorescent neurons, it is not observed for all differentiated fluorescent cell types. The number of morphologically identifiable myocytes that are fluorescent is not reduced by the injection of potassium channel RNA (Fig. 6*B*). In addition, the effect does not appear to be an artifact due to injection of RNA, since it is not observed when similar concentrations of β-galactosidase RNA are coinjected with the fluorescent tracer (Fig. 6*A*, bottom).

Does the effect require a functional potassium channel? This question was addressed by injecting RNA that encodes a mutant potassium channel (Perozo et al., 1993), which induces expression of a channel in oocytes that does not permit ion flux, although gating currents are recorded indicating that protein conformation remains sensitive to changes in membrane voltage. Coinjection of the mutant (WF) RNA with the lineage tracer does not lead to a reduction in the number of fluorescent morphologically identifiable neurons (Fig. 6*A*, bottom). The WF RNA is transcribed from the pBluescript vector (Stratagene), which may interfere with its effectiveness (see Liman et al., 1992), although XSha1 RNA transcribed within a pBluescript context and injected in similar concentrations is still potent (data not shown). Further confirmation of this result was sought by growth in the continued presence of the potassium channel blocker TEA, to titrate away excess potassium channels. Although TEA did appear to rescue neurons in some culture runs, this result was not consistently reproducible. Chronic exposure to TEA has other actions including membrane depolarization (A. B. Ribera, unpublished observations) and enhanced death,

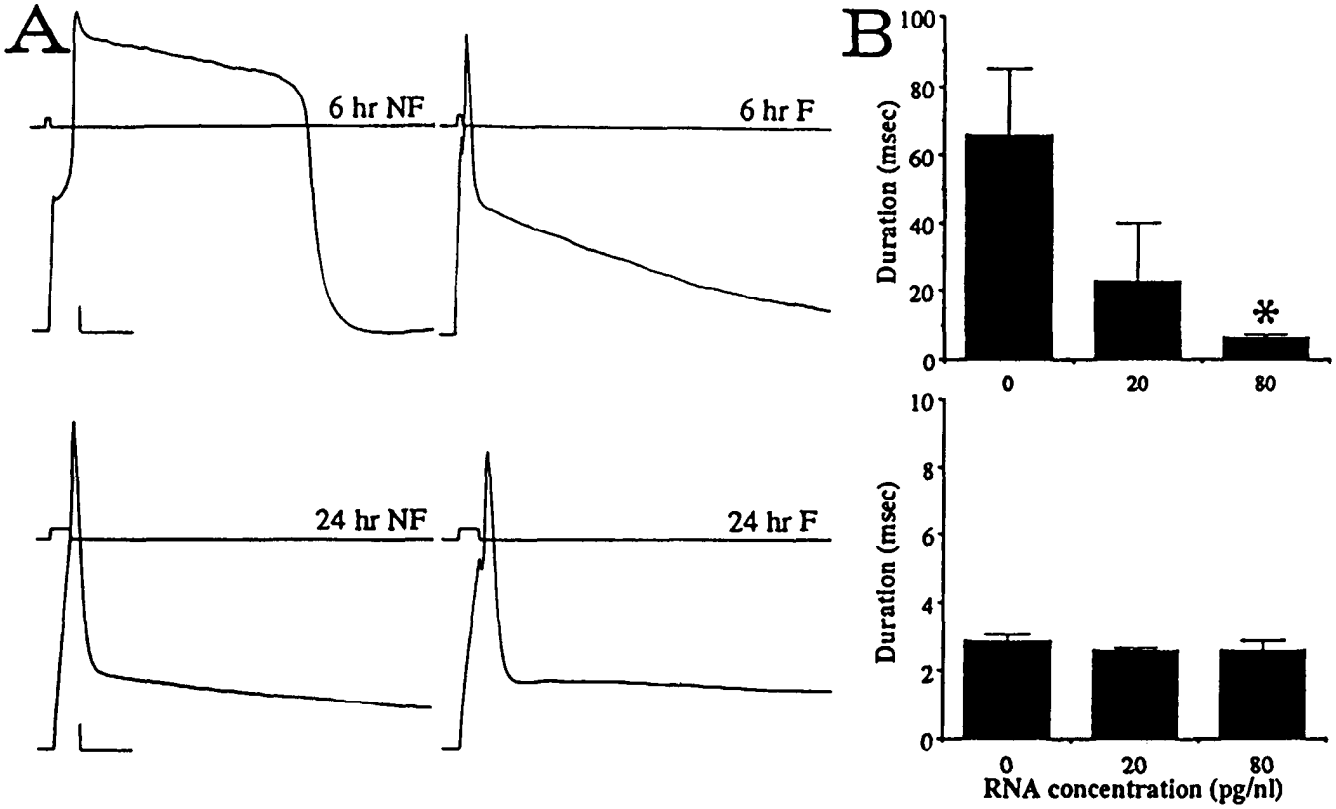

Figure 5. Action potentials are briefer in young fluorescent neurons. *A*, Action potentials recorded from neurons in culture at 6–9 hr in culture (*top*) and 22–26 hr (*bottom*) in culture. In fluorescent neurons (*right*), action potentials are briefer at early but not late times. Neurons were in cultures prepared from embryos injected with 80 pg/nl XShal RNA. Calibration: 10 mV; 20 msec, *top*; 6 msec, *bottom*. The current injection protocol is positioned at 0 mV. *B*, Mean action potential durations at 6–9 hr (*top*) and 22–26 hr (*bottom*) recorded from 4–26 neurons in culture are shown. A concentration of zero refers to data obtained from nonfluorescent neurons. *Asterisk* designates $p \leq 0.03$.

which may interfere with the ability of TEA to block specifically overexpressed potassium channels.

Discussion

We find that increased potassium channel RNA levels result in functional overexpression of potassium currents. The duration of the action potential is shortened, indicating that other currents are not consequently modulated in order to maintain the appropriate impulse duration. Further, there is a dramatic reduction in the appearance of morphologically identifiable neurons.

Relationship between elevated XShal RNA levels and potassium current function

In fluorescent cells that are morphologically identified as neurons, potassium currents are larger by a factor of 2–3 (Fig. 2). However, ~1000 copies of exogenous XShal RNA are expected to be present in an embryonic neuron (see Materials and Methods). Although the delivery of RNA to embryonic neurons appears to be nonuniform (see Fig. 1*A*), it is also possible that higher levels of functional overexpression may promote premature death or suppress neurite initiation (Fig. 6). Since morphological differentiation is required for selection of cells for electrophysiological analysis, such neurons would not have been available for electrophysiological analysis in the present study. The discovery of a marker that identifies neurons using nonmorphological criteria is required for further analysis of this issue.

Potassium current properties and XShal RNA levels in single fluorescent and nonfluorescent neurons could be assessed directly by combining whole-cell recording with reverse transcription–polymerase chain reaction methods (Eberwine et al., 1992).

Table 3. Membrane and recording properties of fluorescent and nonfluorescent neurons

	Young		Mature	
	Fluorescent[a]	Nonfluorescent	Fluorescent[a]	Nonfluorescent
Series resistance (MΩ)	9.6 ± 0.8 (23)	9.0 ± 0.4 (37)	8.2 ± 0.6 (21)	8.3 ± 0.3 (39)
Input resistance (MΩ)	2.1 ± 0.5 (23)	2.8 ± 1.0 (37)	1.4 ± 0.3 (21)	2.1 ± 0.4 (39)
Cell capacitance (pF)	18 ± 1 (23)	22 ± 1 (37)	25 ± 1 (21)	27 ± 1 (39)
Recorded membrane potential (mV)	−38 ± 4 (8)	−44 ± 3 (17)	−49 ± 4 (9)	−47 ± 3 (25)

Numbers in parentheses represent numbers of neurons.

[a] 80 pg/nl injected XShal RNA.

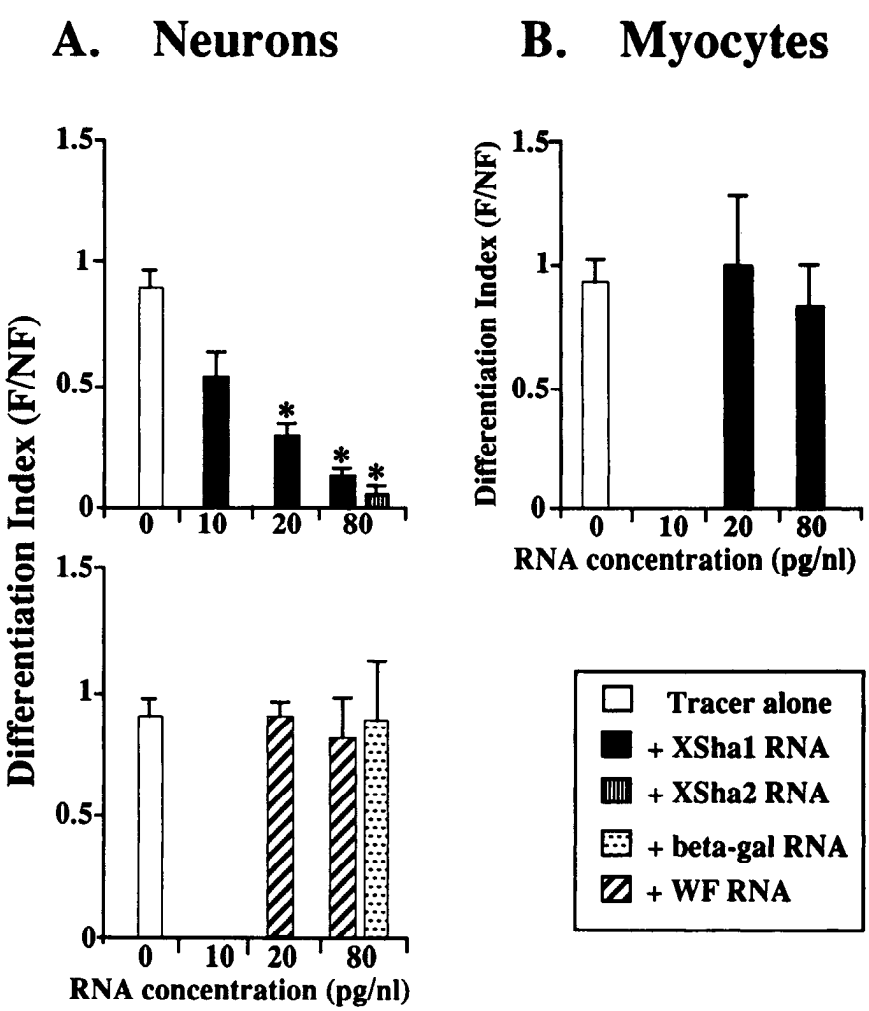

Figure 6. Overexpression of specific RNAs suppresses morphological differentiation of neurons but not myocytes. The differentiation indexes (see Results) calculated for neurons (*A*) and myocytes (*B*) in cultures prepared from embryos injected with indicated RNA and tracer solutions are compared. *A: Top*, Only injection of RNAs encoding functional potassium channels (XSha1 and XSha2) reduces the differentiation index for neurons. Concentrations of 10 and 80 pg/nl represent data pooled from injected doses of 5–10 and 60–80 pg/nl, respectively. *Asterisks* designate $p \leq 0.0001$. *Bottom*, Injection of RNAs encoding β-galactosidase or a mutant potassium channel (WF) does not reduce the differentiation index. For each condition, between 10 and 75 cultures prepared from 3–11 different clutches of embryos were examined. *B*, Injection of XSha1 RNA does not impair morphological differentiation of myocytes. For each condition, between 5 and 14 cultures prepared from two to eight different clutches of embryos were examined.

Since XSha1 peptides translated from injected RNA may assemble with endogenous *Shaker*-like subunits, interpretation of results may not be straightforward. In addition, it is not yet known what other voltage-dependent potassium channel genes are expressed in these neurons (e.g., *Shab, Shal,* and *Shaw*).

Effect of XSha1 RNA overexpression on appearance of morphologically identifiable neurons in culture

The mechanism by which increased levels of potassium channel RNA affect the appearance of morphologically identifiable neurons in culture requires definition. Since it is not known when functional overexpression first occurs, several explanations are possible. Functional overexpression may occur during early cleavage stages, and overactivity of potassium channels may interfere with normal cell divisions and reduce the number of cells contributing to specific lineages. However, the number of morphologically identifiable myocytes is unaffected, suggesting that alterations in the pattern of cell division do not occur in precursors of somitic mesoderm. Alternatively, the efficiency of embryonic inductions may be impaired. For example, membrane receptor–mediated signal transduction plays a role in neural induction and inductive cell–cell interactions (Otte and Moon, 1992; Coffman et al., 1993).

Functional overexpression of potassium currents decreases action potential durations (Fig. 5). Neuronal survival may be compromised by consequent reduction of calcium influx, since intracellular calcium levels are known to influence neuronal survival (Nishi and Berg, 1981; Koike et al., 1989; Collins et al., 1991; Larmet et al., 1992). However, viability probes do not provide evidence that cell death is promoted in cultures prepared from XSha1 injected embryos (data not shown).

Finally, changes in neuronal excitability perturbs aspects of morphological differentiation. For example, innervation of muscle by motor axons in several *Drosophila* excitability mutants is altered; hyperexcitability promotes increased branching, whereas reduced excitability leads to less branching (Budnik et al., 1990). Further, since dynamic levels of intracellular calcium levels influence process outgrowth (Connor, 1986; Cohan et al., 1987; Mattson and Kater, 1987; Bentley et al., 1991; Rehder and Kater, 1992), reduction of impulse duration and consequent calcium influx may alter morphology. However, when grown *in vitro* in the absence of external calcium, *Xenopus* spinal neurons extend longer and thinner processes (Bixby and Spitzer, 1984). These considerations suggest that overexpression of potassium channel RNA would be affecting neurite initiation rather than process outgrowth (see also Holliday and Spitzer, 1993). Primary spinal neurons fire action potentials before neurites initiate (Baccaglini and Spitzer, 1977; Taylor and Roberts, 1983), indicating that excitability has the opportunity to affect initial aspects of morphological differentiation. In contrast, myocyte morphological differentiation is initiated before the onset of their electrical excitability, and the appearance of fluorescent myocytes in culture is not affected by XSha1 RNA overexpression. Examination of dynamic intracellular calcium levels in

fluorescent neurons as well as formation of the nervous system *in situ* will be useful in identifying relevant mechanisms.

Conclusions

The present work evaluates the significance of potassium channel gene transcription in establishing the normal program for electrical excitability. The results demonstrate that, at early times, neurons are capable of expressing more functional potassium channels if RNA levels are elevated. It is also possible that posttranscriptional mechanisms normally restrict translation of potassium channel RNAs to appropriate developmental windows; the lack of 5′ and 3′ untranslated sequences in the injected XSha1 RNA may have eliminated the contribution of this potential regulation. Early overexpression of XSha1 RNA also mimics the developmental changes in kinetic properties of the current (Harris et al., 1988). These findings, taken together with the previous identification of a critical period of RNA synthesis required for potassium current maturation (Ribera and Spitzer, 1989), are consistent with the hypothesis that developmentally regulated levels of potassium channel RNA direct the increase in density of the endogenous delayed-rectifier current. In addition, developmental changes noted in specific properties of whole cell currents (e.g., time to half-maximum) may be brought about by the sequential appearance of new channel subunits. Moreover, the consequences on the action potential of abnormal potassium current differentiation are not compensated by changes in other currents. The inappropriately short impulse durations may suppress or fail to initiate normal developmental cascades.

References

Baccaglini PI, Spitzer NC (1977) Developmental changes in the inward current of the action potential of Rohon-Beard neurones. J Physiol (Lond) 271:93–117.

Baker K, Salkoff L (1990) The *Drosophila Shaker* gene codes for a distinctive K^+ current in a subset of neurons. Neuron 2:129–140.

Barish ME (1986) Differentiation of voltage-gated potassium current and modulation of excitability in cultured amphibian spinal neurones. J Physiol (Lond) 375:229–250.

Bentley D, Guthrie PB, Kater SB (1991) Calcium ion distribution in nascent pioneer axons and coupled preaxonogenesis neurons *in situ*. J Neurosci 11:1300–1308.

Bixby JL, Spitzer NC (1984) Early differentiation of vertebrate spinal neurons in the absence of voltage-dependent Ca^{2+} and Na^+ influx. Dev Biol 106:89–96.

Blair LAC (1983) The timing of protein synthesis required for the development of the sodium action potential in embryonic spinal neurons. J Neurosci 3:1430–1436.

Budnik V, Zhong Y, Wu C-F (1990) Morphological plasticity of motor axons in *Drosophila* mutants with altered excitability. J Neurosci 10: 3754–3768.

Coffman CR, Skoglund P, Harris WA, Kintner CR (1993) Expression of an extracellular deletion of *Xotch* diverts cell fate in *Xenopus* embryos. Cell 73:659–671.

Cohan CS, Connor JA, Kater SB (1987) Electrically and chemically mediated increases in intracellular calcium in neuronal growth cones. J Neurosci 7:3588–3599.

Collins F, Schmidt MF, Guthrie PB, Kater SB (1991) Sustained increase in intracellular calcium promotes neuronal survival. J Neurosci 11:2582–2587.

Connor JA (1986) Digital imaging of free calcium changes and of spatial gradients in growing processes in single, mammalian central nervous system cells. Proc Natl Acad Sci USA 83:6179–6183.

Covarrubias M, Wei AA, Salkoff L (1991) *Shaker, Shal, Shab* and *Shaw* express independent K^+ current systems. Neuron 7:763–773.

Desarmenien MG, Spitzer NC (1991) Role of calcium and protein kinase C in development of the delayed rectifier potassium current in *Xenopus* spinal neurons. Neuron 7:797–805.

Eagleson GW, Harris WA (1990) Mapping of the presumptive brain regions in the neural plate of *Xenopus laevis*. J Neurobiol 21:427–440.

Eberwine J, Yeh H, Miyashiro K, Cao Y, Nair S, Finnell R, Zettel M, Coleman P (1992) Analysis of gene expression in single live neurons. Proc Natl Acad Sci USA 89:3010–3014.

Hamill OP, Marty A, Neher E, Sakmann B, Sigworth FJ (1981) Improved patch-clamp techniques for high resolution current recording from cells and cell-free membrane patches. Pfluegers Arch 391:85–100.

Harland R (1991) *In situ* hybridization: an improved whole-mount method for *Xenopus* embryos. In: Methods in cell biology, Vol 36, *Xenopus laevis* (Kay B, Peng B, eds), pp 685–695. San Diego: Academic.

Harland R, Mischer L (1988) Stability of RNA in developing *Xenopus* embryos and identification of a destabilizing sequence in TFIIIA messenger RNA. Development 102:837–852.

Harris GL, Henderson LP, Spitzer NC (1988) Changes in densities and kinetics of delayed rectifier potassium channels during neuronal differentiation. Neuron 1:739–750.

Hartenstein V (1989) Early neurogenesis in *Xenopus*: the spatio-temporal pattern of proliferation and cell lineages in the embryonic spinal cord. Neuron 3:399–411.

Haugland FN, Wu C-F (1990) A voltage-clamp analysis of gene-dosage effects of the *Shaker* locus on larval muscle potassium currents in *Drosophila*. J Neurosci 10:1357–1371.

Henderson LP, Spitzer NC (1986) Autonomous early differentiation of neurons and muscle cells in single cell cultures. Dev Biol 113:381–387.

Henderson LP, Smith MA, Spitzer NC (1984) The absence of calcium blocks impulse-evoked release of acetylcholine but not *de novo* formation of functional neuromuscular synaptic contacts in culture. J Neurosci 4:3140–3150.

Holliday J, Spitzer NC (1990) Spontaneous calcium influx and its roles in differentiation of spinal neurons in culture. Dev Biol 141:13–23.

Holliday J, Spitzer NC (1991) Calcium channels in the regulation of cell development and cellular interactions. In: Calcium channels: their properties, functions, regulation, and clinical relevance (Hurwitz L, Partridge LD, Leach JK, eds), pp 137–155. Boca Raton: CRC.

Holliday J, Spitzer NC (1993) Interactions between myocytes and extracellular calcium that affect the differentiation of cultured neurons. J Neurobiol 24:506–514.

Holliday J, Adams RJ, Sejnowski TJ, Spitzer NC (1991) Calcium-induced release of calcium regulates differentiation of cultured spinal neurons. Neuron 7:786–796.

Jan LY, Jan YN (1992) Structural elements involved in specific K^+ channel functions. Annu Rev Physiol 54:537–555.

Kaang B-K, Pfaffinger PJ, Grant SG, Kandel ER, Furukawa Y (1992) Overexpression of an *Aplysia Shaker* K^+ channel gene modifies the electrical properties and synaptic efficacy of identified *Aplysia* neurons. Proc Natl Acad Sci USA 89:1133–1137.

Kintner C (1988) Effects of altered expression of the neural cell adhesion molecule, N-CAM, on early neural development in *Xenopus* embryos. Neuron 1:545–555.

Klein SJ (1987) The first cleavage furrow demarcates the dorsal-ventral axis in *Xenopus* embryos. Dev Biol 120:299–304.

Koike T, Martin DP, Johnson EM Jr (1989) Role of Ca^{2+} channels in the ability of membrane depolarization to prevent neuronal death induced by trophic-factor deprivation: evidence that levels of internal Ca^+ determine nerve growth factor dependence of sympathetic ganglion cells. Proc Natl Acad Sci USA 86:6421–6425.

Lamborghini JE (1980) Rohon-Beard cells and other large neurons in *Xenopus* embryos originate during gastrulation. J Comp Neurol 189: 323–333.

Larmet Y, Dolphin AC, Davies AM (1992) Intracellular calcium regulates the survival of early sensory neurons before they become dependent on neurotrophic factors. Neuron 9:563–574.

Liman ER, Tytgat J, Hess P (1992) Subunit stoichiometry of a mammalian K^+ channel determined by construction of multimeric cDNAs. Neuron 9:861–871.

Lockery SR, Spitzer NC (1992) Reconstruction of action potential development from whole cell currents of differentiating spinal neurons. J Neurosci 12:2268–2287.

Lu B, Greengard P, Poo M-M (1992) Exogenous synapsin I promotes functional maturation of developing neuromuscular synapses. Neuron 8:521–529.

Mattson MP, Kater SB (1987) Calcium regulation of neurite elongation and growth cone motility. J Neurosci 7:4034–4043.

Melton DA, Krieg PA, Rebagliati MR, Maniatis T, Zinn K, Green MR (1984) Efficient *in vitro* synthesis of biologically active RNA and RNA hybridization probes from plasmids containing a bacteriophage SP6 promoter. Nucl Acids Res 12:7035–7056.

Moon RT, Christian J (1989) Microinjection and expression of synthetic mRNAs in *Xenopus* embryos. Technique 1:76–89.

Nieuwkoop PD, Faber J (1967) Normal table of *Xenopus laevis*. Amsterdam: North Holland.

Nishi R, Berg DK (1981) Effects of high K^+ concentrations on the growth and development of ciliary ganglion neurons in culture. Dev Biol 87:301–307.

O'Dowd DK (1983) RNA synthesis dependence of action potential development in spinal cord neurones. Nature 303:619–621.

O'Dowd DK, Ribera AB, Spitzer NC (1988) Development of voltage-dependent calcium, sodium and potassium currents in *Xenopus* spinal neurons. J Neurosci 8:792–805.

Otte AP, Moon RT (1992) Protein kinase C isozymes have distinct roles in neural induction and competence in *Xenopus*. Cell 68:1021–1029.

Perozo E, MacKinnon R, Bezanilla F, Stefani E (1993) Gating currents from a nonconducting mutant reveal open-closed conformations in *Shaker* K^+ channels. Neuron 11:353–358.

Rehder V, Kater SB (1992) Regulation of growth cone filopodia by intracellular calcium. J Neurosci 12:3175–3186.

Ribera AB (1990) A potassium channel gene is expressed at neural induction. Neuron 5:691–701.

Ribera AB, Nguyen D-A (1993) Primary sensory neurons express a *Shaker* like potassium channel gene. J Neurosci 13:4988–4996.

Ribera AB, Spitzer NC (1989) A critical period of transcription required for differentiation of the action potential of spinal neurons. Neuron 2:1055–1062.

Ribera AB, Spitzer NC (1991) The differentiation of potassium current in embryonic amphibian myocytes. Dev Biol 144:119–128.

Ribera AB, Spitzer NC (1992) Developmental regulation of potassium channels and the impact on neuronal differentiation. In: Ion channels, Vol 3 (Narahashi T, ed), pp 1–38. New York: Plenum.

Salkoff L, Baker K, Butler A, Covarrubias M, Pak MD, Wei A (1992) An essential 'set' of K^+ channels conserved in flies, mice and humans. Trends Neurosci 15:161–166.

Sheng M, Tsaur M-L, Jan YN, Jan LY (1992) Subcellular segregation of two A-type K^+ channel proteins in rat central neurons. Neuron 9:271–284.

Spitzer NC (1994) Spontaneous calcium spikes and waves in embryonic neurons: signaling systems for differentiation. Trends Neurosci, in press.

Spitzer NC, Lamborghini JE (1976) The development of the action potential mechanism of amphibian neurons isolated in cell culture. Proc Natl Acad Sci USA 73:1641–1645.

Taylor JSH, Roberts A (1983) The early development of the primary sensory neurones in an amphibian embryo: a scanning electron microscope study. J Embryol Exp Morphol 75:49–66.

Timpe LC, Jan LY (1987) Gene dosage and complementation analysis of the *Shaker* locus in *Drosophila*. J Neurosci 7:1307–1317.

Warner AE (1973) The electrical properties of the ectoderm in the amphibian embryo during induction and early development of the nervous system. J Physiol (Lond) 235:267–286.

Wu R-L, Barish ME (1992) Two pharmacologically and kinetically distinct transient potassium currents in cultured embryonic mouse hippocampal neurons. J Neurosci 12:2235–2246.